Received: 6 February 2024 | Revised: 1 March 2024 | Accepted: 3 March 2024
DOI: 10.1002/pc.28317

RESEARCH ARTICLE

Polymer COMPOSITES WILEY

Tribological behavior and mechanism of $Mo_2Ti_2C_3$/polyimide composite films under dry friction condition

Xinrui Wang[1] | Guojing Chen[1] | Yufei Huang[1] | Zhenqian Ma[1] | Xuan Yin[2] | Chunpeng Chai[1]

[1]School of Materials Science and Engineering, Beijing Institute of Technology, Beijing, China

[2]College of Mechanical and Electrical Engineering, Beijing University of Chemical Technology, Beijing, China

Correspondence
Chunpeng Chai, School of Materials Science and Engineering, Beijing Institute of Technology, Beijing 100081, China.
Email: chaicp@bit.edu.cn

Abstract

Polyimide (PI) has good mechanical properties and thermal stability, while high coefficient (COF) and wear rate limit its wide application. In order to endow PI with better friction and wear resistance, $Mo_2Ti_2C_3$ MXene was used as solid lubricant to prepare $Mo_2Ti_2C_3$/PI nanocomposites with different content of $Mo_2Ti_2C_3$. The effect of the amount of $Mo_2Ti_2C_3$ on the tribological behavior of PI was explored and the tribological mechanism was also analyzed Tribological tests showed that at 1.2 wt% of $Mo_2Ti_2C_3$ addition, the composite material demonstrated superior friction and wear resistance, exhibiting a 19.9% decrease in the COF and a 79.7% decrease in the wear rate compared to single PI due to the good self-lubricating properties of $Mo_2Ti_2C_3$ MXene. Moreover, $Mo_2Ti_2C_3$ can also effectively assist PI to form sleek transfer films without interruption or gaps on the steel balls, resulting in a reduced friction COF and wear rate of the material. This work demonstrates that $Mo_2Ti_2C_3$ MXene is an aussichtsreich additive for polymers to improve the tribological properties and broadens the applications of $Mo_2Ti_2C_3$/PI composites in friction material area.

Highlights

- $Mo_2Ti_2C_3$ significantly improves the tribological performance of polyimide.
- The thermal properties of $Mo_2Ti_2C_3$/polyimide are enhanced by the introduction of $Mo_2Ti_2C_3$.
- The minimum coefficient of $Mo_2Ti_2C_3$/PI composites was only 0.246 at the 1.2 wt% content of $Mo_2Ti_2C_3$.
- The wear rate of $Mo_2Ti_2C_3$/PI composites was decreased by 79.7% at the 1.2 wt% addition of $Mo_2Ti_2C_3$.
- $Mo_2Ti_2C_3$ promotes the establishment of tribo-film to protect the $Mo_2Ti_2C_3$/PI composites from friction.

KEYWORDS

lubrication mechanism, $Mo_2Ti_2C_3$ MXene, polyimide, tribological properties

Xinrui Wang and Guojing Chen contributed equally to this work.

1 | INTRODUCTION

Polyimide (PI) has the advantages of excellent thermal stability, good anticorrosion ability, good mechanical properties, self-lubrication property, and so forth.[1,2] PI film can be used as the lubrication film on the surface of gear, compressor, bearing and other tribological parts, widely involved in aerospace, marine engineering, machinery equipment and automobile industry.[3,4] However, single PI also has the defect of high coefficient (COF) and wear rate. In addition, complex friction conditions such as high contact stress and different sliding speeds may seriously deteriorate the tribological behaviors of single PI films.[5] Therefore, it is very important to enhance the tribological behaviors of PI under diversiform friction conditions.

Compounding two-dimensional layered solid lubrication materials such as graphene, disulphide and carbon nitride with the PI matrix is one of the resultful ways to ameliorate the tribological behaviors of PI. Yang et al.[6] fabricated thermosetting PI composite with MoS_2 as lubricating filler. Because of the good self-lubrication property and high crystallization of layered MoS_2, transfer films would be formed during the sliding process, preventing the composite from the long-time direct contact with the counterface during the sliding and finally ameliorate the tribological behaviors. The COF of the MoS_2/PI composite reached the lowest (0.11) when the additive amount of MoS_2 got to 20 wt% and the wear loss is only a quarter of single PI under this formulation. Zhu et al.[7] prepared g-C_3N_4/PI composites with a sequence of proportion. Scanning electron microscope (SEM) results showed that the wear type transformed into abrasive wear from adhesive wear after the addition of two-dimensional layered material g-C_3N_4. When the g-C_3N_4 filler entered the furrow during friction, it reduced the roughness of the wear counterface and formed a continuous transfer film that reduced the COF and wear rate. By the time the additive amount of g-C_3N_4 filler reached 10 wt%, the g-C_3N_4/PI composite had the best tribological performances. Previous researches have shown that the tribological behaviors of PI matrix could be significantly enhanced by introducing two-dimensional layered solid lubrication materials into the matrix. However, two-dimensional layered solid lubrication materials currently studied have many problems, for example, the lack of surface functional groups, easy to agglomerate, poor compatibility with matrix and other problems. As a result, it is necessary to functionalize the surface of the materials. Min et al.[8] prepared amine-functionalized graphene nanosheets (AGNS)/PI composites films. On account of the good chemical compatibility and the strong interfacial adhesion between AGNS and PI, the tribological behaviors of PI could be observably improved, and the abrasion marks on the surface of the composites could be shallower and narrower. The addition of only 0.5 wt% of AGNS reduced the COF and wear rate of the composite by about 41.9% and 72.6%. The modified two-dimensional laminated material after functionalization can certainly improve the compatibility with the body, but it will increase the treatment process and cost.

MXene is a novel transition metal carbon/nitrogen compound synthesized by Naguib et al.[9] in 2011. It is a two-dimensional layered material with an abundance of functional groups for instance —F, —O, and —OH on the surface.[10] MXene possesses a unique lamellar structure, and between the lamellae exists weak van der Waals' forces, leading to good self-lubrication property that is promising for improving polymer tribological properties. Meng et al.[11] used freeze-drying method to obtain Ti_3C_2 MXene nanosheets with three-dimensional lattices, and prepared epoxy- Ti_3C_2 3DNS composites. Ti_3C_2 MXene were prone to produce flaky debris during friction. Some of the debris existing between the friction pairs were compacted and some of them are sliding, providing good lubricating impact. The concentration of nanosheets of 1 g could lessen the COF by 76.3% and wear rate by 67.3%. Bashandeh et al.[12] prepared MXene nanosheet-reinforced aromatic thermoset co-polyester (ATSP) wear-resistant composites, and 5 wt% MXene/ATSP was experimentally measured to have the minimum COF of 0.12. Yin et al.[13] utilized Polyamide acid (PAA) composites with MXene to construct PAA-co-MXene-modified PLC films, and found that the low molecular weight 0.45 MPAA-co-MXene composite film was able to rapidly form an oxygen-rich carbon friction layer during sliding, which reduced the COF and the wear rate to 0.21 and 1.5×10^{-6} mm^3 N^{-1} m^{-1}, respectively. The above studies proved that the addition of MXene could evidently enhance the tribological behaviors of polymer matrix. In recent years, density functional theory has forecast that $Mo_2Ti_2C_3$ and other Mo-based well-organized double transition metal carbides MXenes also have lamellar structures. These MXenes have hexagonal crystal structure and large interlamellar spacing, possessing excellent electrochemical and chemical properties.[14] Besides, previous studies have proven that the oxides of Mo have good self-lubricating properties.[15] Therefore, we expect that the tribological behaviors of PI matrix could be significantly improved by the incorporation of $Mo_2Ti_2C_3$ over the conventional Ti_3C_2 MXene.

In this study, the tribological performances of PI were ameliorated by adding $Mo_2Ti_2C_3$ MXene as solid lubricant to the PI matrix. The multilayer $Mo_2Ti_2C_3$ MXene powder was obtained from $Mo_2Ti_2C_3$ MAX by HF etching. PAA was prepared by amidation reaction between 4,4′-oxydianiline (ODA) and 3,3′,4,4′-Biphenyl tetracarboxylic

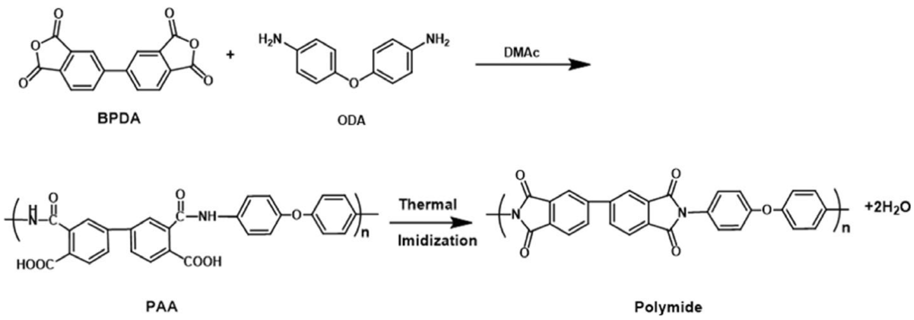

FIGURE 1 The chemical reaction for the synthesis of polyimide.

diandhydride (BPDA). $Mo_2Ti_2C_3$ MXene was blended with PAA to obtain $Mo_2Ti_2C_3$/PAA suspension, and flexible $Mo_2Ti_2C_3$/PI nanocomposite films were prepared by drying and thermal imidization. The tribological performances of flexible $Mo_2Ti_2C_3$/PI nanocomposite films were carried out by a multi-function ball-on-disk tribometer. The wear mechanism was investigated using 3D white light interferometer and x-ray photoelectron spectroscopy (XPS). The optimal amount of $Mo_2Ti_2C_3$ MXene added was determined through the above experiments, which affords an original way for the design of friction and wear-resistant materials.

2 | EXPERIMENTAL SECTION

2.1 | Materials

ODA powder was supplied by Energy Chemical, China. BPD powder was supplied by Meryer, China. *N,N*-Dimethylacetamide (DMAc) was supplied by Jindongtianzheng Precision Chemical Reagent Factory, China. $Mo_2Ti_2AlC_3$ MAX phase powder was supplied by Beike Nano, China. Hydrofluoric acid (HF) was supplied by Titan Scientific, China.

2.2 | Preparation of $Mo_2Ti_2C_3$ MXene

$Mo_2Ti_2C_3$ MXene powder was synthesized by selective etching of aluminum layers of $Mo_2Ti_2AlC_3$. The synthesis procedure was in line with previous works.[14,16] First, 1 g of $Mo_2Ti_2AlC_3$ powder was gradually added to 10 mL of 50% HF. Then, the suspension was magnetically stirred at 60°C and 500 rpm for 96 h. Deionized (DI) water was added to the suspension and centrifuged at 3500 rpm for 5 min. This procedure was repeated until the supernatant liquid reached neutral. The obtained multilayered $Mo_2Ti_2C_3$ sediment was dispersed in DI water for 2 h under ultrasonication and was centrifuged for 1 h at 3500 rpm. Strain and then freeze dry for 48 h to obtain $Mo_2Ti_2C_3$ MXene powder.

2.3 | Preparation of $Mo_2Ti_2C_3$/PI nanocomposite films

Figure 1 displays the chemical reaction of the synthesis of PI. ODA and appropriate amount of DMAc were put into a flask, and ultrasonically dispersed at room temperature until ODA was completely dissolved and then stirred for 20 min at room temperature (25°C). BPDA was added in three batches, and PAA was obtained by stirring for 3 h. $Mo_2Ti_2C_3$ was mixed with DMAc, and ultrasonically dispersed for 30 min, and then mixed with PAA and stirred magnetically for 30 min at room temperature. The $Mo_2Ti_2C_3$/PAA complex was uniformly coated on a 20 mm × 20 mm steel plate, dried at 70°C under vacuum for 7 h to separate out the solvent, and finally put in a tube furnace programmed to raise the temperature to 300°C for thermal imidization to prepare flexible $Mo_2Ti_2C_3$/PI nanocomposite films. In this work, single PI, 0.4 wt% $Mo_2Ti_2C_3$/PI, 0.8 wt% $Mo_2Ti_2C_3$/PI, 1.2 wt% $Mo_2Ti_2C_3$/PI, 1.6 wt% $Mo_2Ti_2C_3$/PI and 2.0 wt% $Mo_2Ti_2C_3$/PI composite films were prepared. The above samples were named PI, MTPI-1∼5, respectively.

2.4 | Friction and wear experiments

The friction and wear experiments were investigated on a multi-function ball-on-disc tribometer (BOD, MS-M9000, China). The tests were performed under dryly with 20 min, constant load of 3 N, rotational speed of 300 r/min, rotational radius of 3 mm. The steel balls with a diameter of 4 mm used for the tribological experiments were made of GCr15 bearing steel. The balls were washed with anhydrous ethanol and dried before each experiment. The samples were settled on a stainless-steel circular disc base for tribological experiments (Figure 2). To acquire the mean COF and wear rate, three replicate experiments were performed for each sample.

The wear rates were calculated by the equation:

$$W = \frac{V}{F \times L}$$

where W ($mm^3/(m\ N)$) indicates wear rate, V (mm^3) indicates the volume of scratches that can be given by the 3D white light interferometer, F (N) indicates the constant load applied in the tests, and L (m) is whole sliding distance.

3 | RESULTS AND DISCUSSION

3.1 | Microstructure characterization of $Mo_2Ti_2C_3$ MXene

In order to prove the successful preparation of $Mo_2Ti_2C_3$, we performed SEM characterization of $Mo_2Ti_2AlC_3$ and $Mo_2Ti_2C_3$, and the consequences are exhibited in Figure 3A,B. From Figure 3A, we can see that $Mo_2Ti_2AlC_3$ has a close-packed layer morphology, and the interlamellar spacing becomes larger after etching, showing a layer-by-layer accordion morphology with different interlayer distances. To obtain the lattice structure information of $Mo_2Ti_2C_3$, we carried out x-ray diffraction (XRD) characterization of $Mo_2Ti_2C_3$. The result of XRD test is exhibited in Figure 3C. In the XRD pattern, the (002) characteristic diffraction peak attributes to the typically characteristic diffraction peak of $Mo_2Ti_2C_3$.[17]

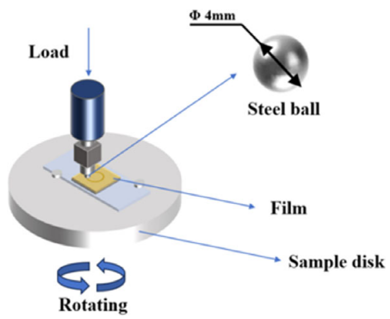

FIGURE 2 Diagrammatic sketch of friction and wear tests.

The surface chemical elemental states of the elemental $Mo_2Ti_2C_3$ were characterized by XPS. The XPS full spectrum measurements of $Mo_2Ti_2C_3$ are shown in Figure 3D. From it, we can see the existence of elements C, O, Mo, and Ti on $Mo_2Ti_2C_3$. In addition, the fine spectra of Ti 2p, Mo 3d of $Mo_2Ti_2C_3$ are exhibited in Figure 3E,F. The fine spectrum of Ti 2p showed in Figure 3E was deconvoluted into Ti-C $2p_{3/2}$ at 458.9 eV, Ti^{2+} $2p_{3/2}$ at 459.6 eV, Ti^{3+} $2p_{3/2}$ at 460.7 eV, TiO_2 $2p_{3/2}$ at 462.6 eV, Ti^{2+} $2p_{1/2}$ at 464.5 eV, Ti-C $2p_{1/2}$ at 464.9 eV, Ti^{3+} $2p_{1/2}$ at 466.0 eV, TiO_2 $2p_{1/2}$ at 467.5 eV, respectively.[18] The XPS fine spectrum of Mo 3d (Figure 3F) was deconvoluted into Mo-C at 228.0 eV, Mo^{4+} $3d_{5/2}$ at 230.4 eV, Mo^{6+} $3d_{5/2}$ at 232.1 eV, Mo^{5+} $3d_{5/2}$ at 233.1 eV, Mo^{6+} $3d_{3/2}$ at 235.3 eV, and Mo^{5+} $3d_{3/2}$ at 236.2 eV.[14]

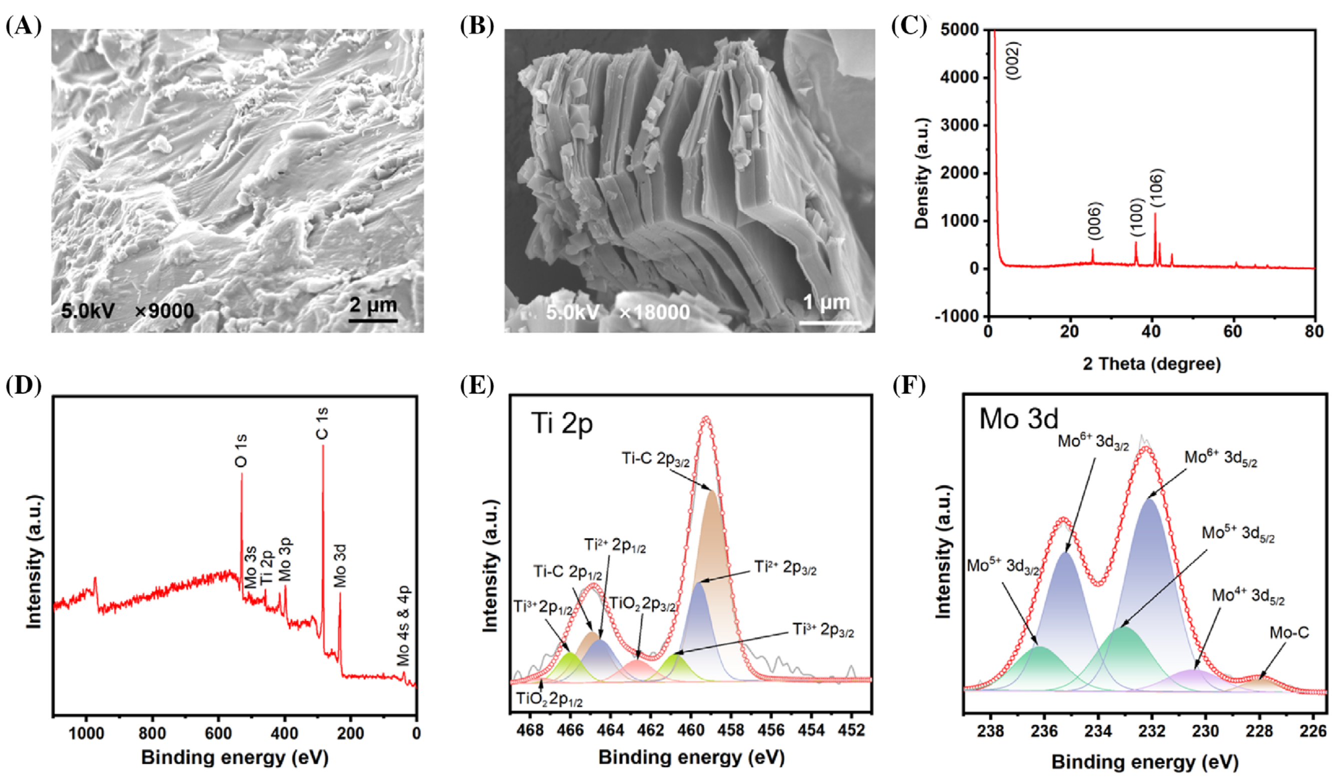

FIGURE 3 Scanning electron microscope images of (A) $Mo_2Ti_2AlC_3$ and (B) $Mo_2Ti_2C_3$; x-ray diffraction (C) pattern of $Mo_2Ti_2C_3$; x-ray photoelectron spectroscopy (D–F) profiles of $Mo_2Ti_2C_3$.

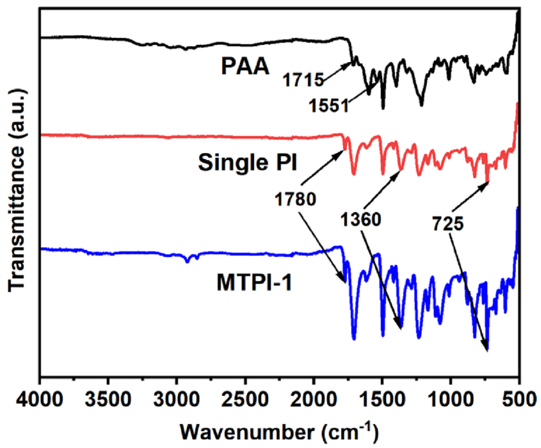

FIGURE 4 Fourier transform infrared spectroscopy spectra of PAA, PI and MTPI-1.

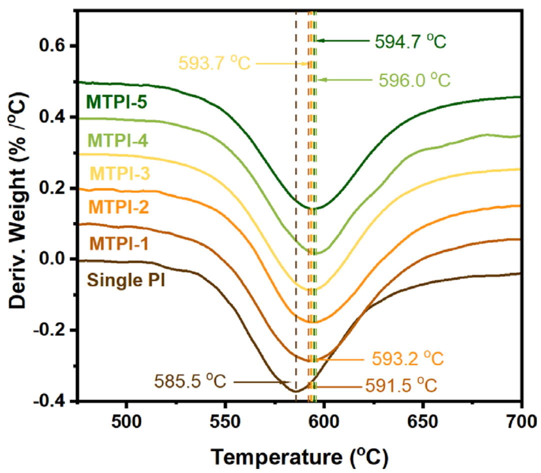

FIGURE 5 DTG curves of single polyimide and MTPI-1∼5.

Among them, Mo^{6+} and Ti^{3+} are the main oxidation states of Mo and Ti in $Mo_2Ti_2C_3$.

3.2 | Structure and properties of $Mo_2Ti_2C_3$/PI composites

Fourier transform infrared spectroscopy (FT-IR) spectroscopy was implemented so as to investigate the chemical construction of PI as well as $Mo_2Ti_2C_3$/PI composites. The FT-IR spectra of PAA, PI and MTPI-1 are displayed in Figure 4. Observing the PAA spectrum, we can see that the absorption bands at 1715 and 1551 cm^{-1} correspond to the bending vibration of the —COOH functional group and the stretching vibration of the —NH functional group, respectively.[19] For PI and MTPI-1, the above PAA characteristic peaks disappeared, and the absorption peak at 1780 cm^{-1} corresponded to the stretching vibration of symmetric C═O. The absorption peak at 725 cm^{-1} corresponded to the bending vibration of C═O in the acylimide ring, which was the characteristic peak of the acylimide functional group, representing that PAA had been successfully thermally iminated. Meanwhile, the C—N stretching vibration at 1360 cm^{-1} indicated that the polyimide was successfully prepared.[20]

For the sake of investigating the effect of $Mo_2Ti_2C_3$ MXene on the thermal properties of PI, we performed TGA tests of single PI and $Mo_2Ti_2C_3$/PI composites in N_2, and the results of the tests are shown in Figure 5. There is almost no weight loss of single PI and $Mo_2Ti_2C_3$/PI composites up to 500°C, which proves that the materials have a better thermal stability and the addition of the filler did not have any significant effect on the thermal decomposition mechanism of the materials. From the DTG data, the maximum decomposition temperature of single PI is 585.5°C. With the addition of $Mo_2Ti_2C_3$, the maximum decomposition temperature of $Mo_2Ti_2C_3$/PI composites increased gradually. Among them, the maximum decomposition temperature of MTPI-4 was the highest, which was 596°C. This is because the mixing of $Mo_2Ti_2C_3$ with PI blocks the motion of the main chain of PI molecules, increases the fracture energy of molecular chain relaxation, and increases the thermal decomposition temperature.[21] At the same time, the unique lamellar structure of $Mo_2Ti_2C_3$ facilitates heat transfer and can avoid localized accumulation of heat. However, when the content of $Mo_2Ti_2C_3$ is too high, its dispersion in the PI matrix becomes poor, leading to poor thermal stability of the composite.[22] In summary, the addition of moderate amount of $Mo_2Ti_2C_3$ could evidently improve the thermal properties of PI.

3.3 | Friction and wear properties of $Mo_2Ti_2C_3$/PI composites

The tribological performances of single PI and $Mo_2Ti_2C_3$/PI composites with various $Mo_2Ti_2C_3$ contents were comparatively investigated under the conditions of the constant load of 3 N and rotational speed of 300 r/min, and results are displayed in Figure 6. Adding $Mo_2Ti_2C_3$ into PI can significantly reduce the COF and the wear rate of single PI, decreasing gradually as the content of $Mo_2Ti_2C_3$ increased. When the content of $Mo_2Ti_2C_3$ reached 1.2 wt%, the COF and wear rate reached the lowest at 0.246 and 1.460, respectively. Thereafter the COF and wear rate of the composites increased in the wake of the concentration of $Mo_2Ti_2C_3$ continued to increase. The $Mo_2Ti_2C_3$ material has good self-lubrication, and the partially exfoliated flake layer is favorable to form a continuous transfer film on the friction counterface during the sliding procedure. However, if the content of $Mo_2Ti_2C_3$ is too high, it

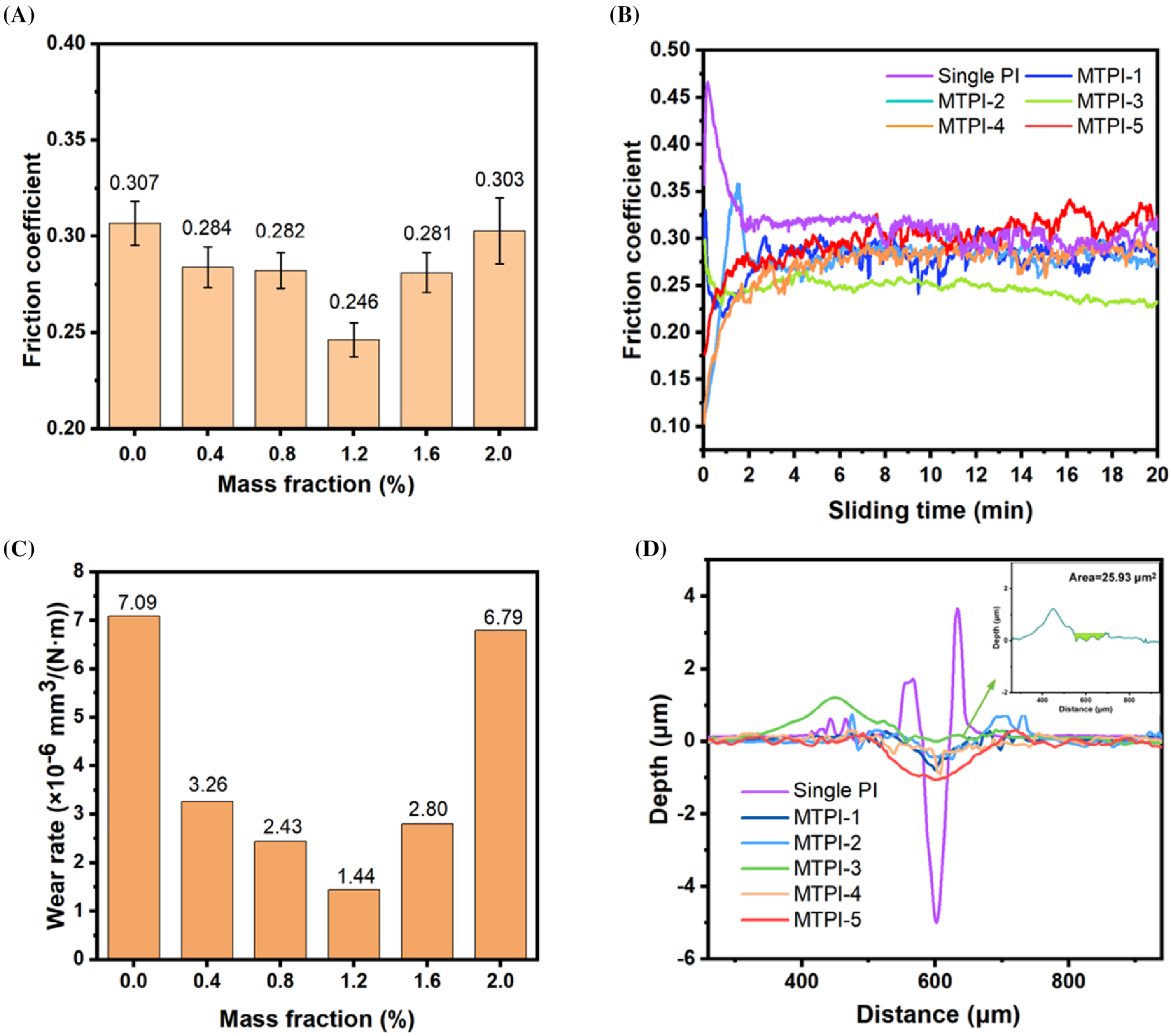

FIGURE 6 Tribological properties of $Mo_2Ti_2C_3$/PI samples (A) coefficient (COF) of single PI and MTPI-1∼5; (B) variation of COF of single PI and MTPI-1∼5 with sliding time; (C) average wear rates of single PI and MTPI-1∼5; (D) distance-depth curves of abrasion marks for single PI and MTPI-1∼5.

will be partially agglomerated, which increases the hardness of the abrasive chips and worsens the tribological performances.

Furthermore, the variation of COF of single PI and $Mo_2Ti_2C_3$/PI depending on sliding time is exhibited in Figure 6B. During the beginning stage of the sliding process, the distinct contact surface between the steel balls and the composites was small, and the COF of single PI and $Mo_2Ti_2C_3$/PI composites increased. Plastic deformation occurred because of shear stress. Especially, single PI is susceptible to plastic deformation. As a result, its COF rose rapidly at the initial stage.[23] After the addition of $Mo_2Ti_2C_3$, the plastic deformation of the sample while sliding is decreased due to the reinforcing effect of $Mo_2Ti_2C_3$ on PI, so that the increase of COF during the initial stage of friction is reduced and the COF is more stable. The tribological properties of the $Mo_2Ti_2C_3$/PI composites prepared in this paper are superior, specifically, the COF and wear rate are lower than the data of these samples in the recently published articles in this field (Table 1). Therefore, $Mo_2Ti_2C_3$ can effectively improve the tribological properties of PI and is a solid lubricant with potential applications in polymer friction.

The transfer films and abrasive spots' morphology on the steel balls' surface as well as the morphology of the abrasive marks on the wear surface were observed with a

TABLE 1 Comparison of the tribological properties of this paper with other literatures.

Refs.	24	25	26	27	28	29	This work
COF	0.27	0.33	0.31	0.31	0.32	0.51	0.25
Wear rate $\times 10^{-5}$	1.78	0.24	0.20	0.39	0.62	0.47	0.14

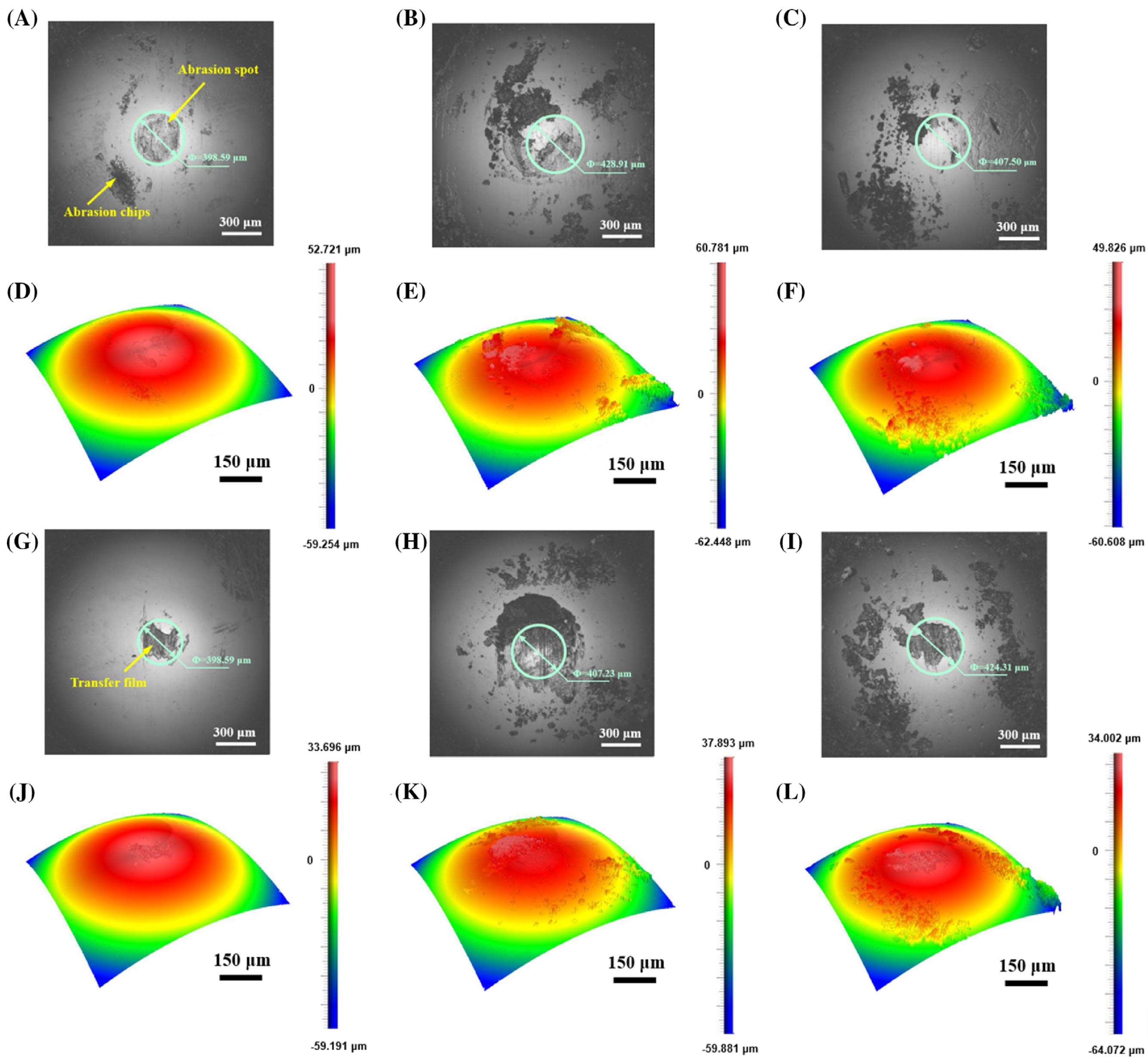

FIGURE 7 White light interferometric fringing intensity map (A–C), (G–I) and 3D morphology (D–F), (J–L) of the surface of steel balls: (A, D) single PI; (B, E): MTPI-1; (C, F): MTPI-2; (G, J): MTPI-3; (H, K): MTPI-4; (I, L): MTPI-5.

3D white light interferometry. As shown in Figures 7 and 8, single PI formed more abrasive chips adhering to the surface of the steel ball while sliding, and there were numerous grooves along the sliding direction on the steel ball. The abrasion mark on the wear surface was deep and have obvious grooves. This is due to the severe abrasive wear between the abrasive chips generated by friction and the softer PI substrate, resulting in the formation of deep grooves. When a small amount of $Mo_2Ti_2C_3$ was added, the tribological properties of the composites were slightly improved, but the $Mo_2Ti_2C_3$ exposed to the wear surface caused the wear spots on the friction surface to increase, thus showing that the wear spots of MTPI-1 and MTPI-2 were larger than those of PI (Figure 7A–F). The tribological properties of the samples were optimized when the addition of $Mo_2Ti_2C_3$ reached the optimum value

(Figure 7G,J). Once the addition of $Mo_2Ti_2C_3$ exceeds the optimum value, the tribological properties of the composites decrease, which is manifested by the increase of the abrasive spots (Figure 7H,I,K,L). The experimental results in Figure 6 correspond to the wear spot results in Figure 7. In the wake of the increase of $Mo_2Ti_2C_3$ concentration, the wear condition on the wear surface was alleviated and a smoother transfer film gradually came into being. The wear surface area was smooth, while the grooves became shallow, and the wear form changed to slight abrasive wear and adhesive wear.[30] When the content of $Mo_2Ti_2C_3$ reached 1.2 wt%, a smooth and continuous transfer film was formed on the steel ball, with the smallest area of abrasion spot and fewer abrasion chips. The abrasion marks on the wear surface were the shallowest and narrowest in width, which further proved that the composites with the addition of 1.2 wt% $Mo_2Ti_2C_3$ had the best tribological properties. When the content of $Mo_2Ti_2C_3$ exceeded 1.2 wt%, the abrasion chips increased. The grooves on the steel ball became more obvious. The samples produced a large number of stripping and stuck to steel ball, and the abrasion marks widen and the grooves became deeper. This is due to the excessive $Mo_2Ti_2C_3$ in the PI matrix is not easy to distribute uniformly,[31] prone to agglomeration. As a consequence, the friction surface becomes rougher, exacerbating the abrasive wear, so that the COF and the

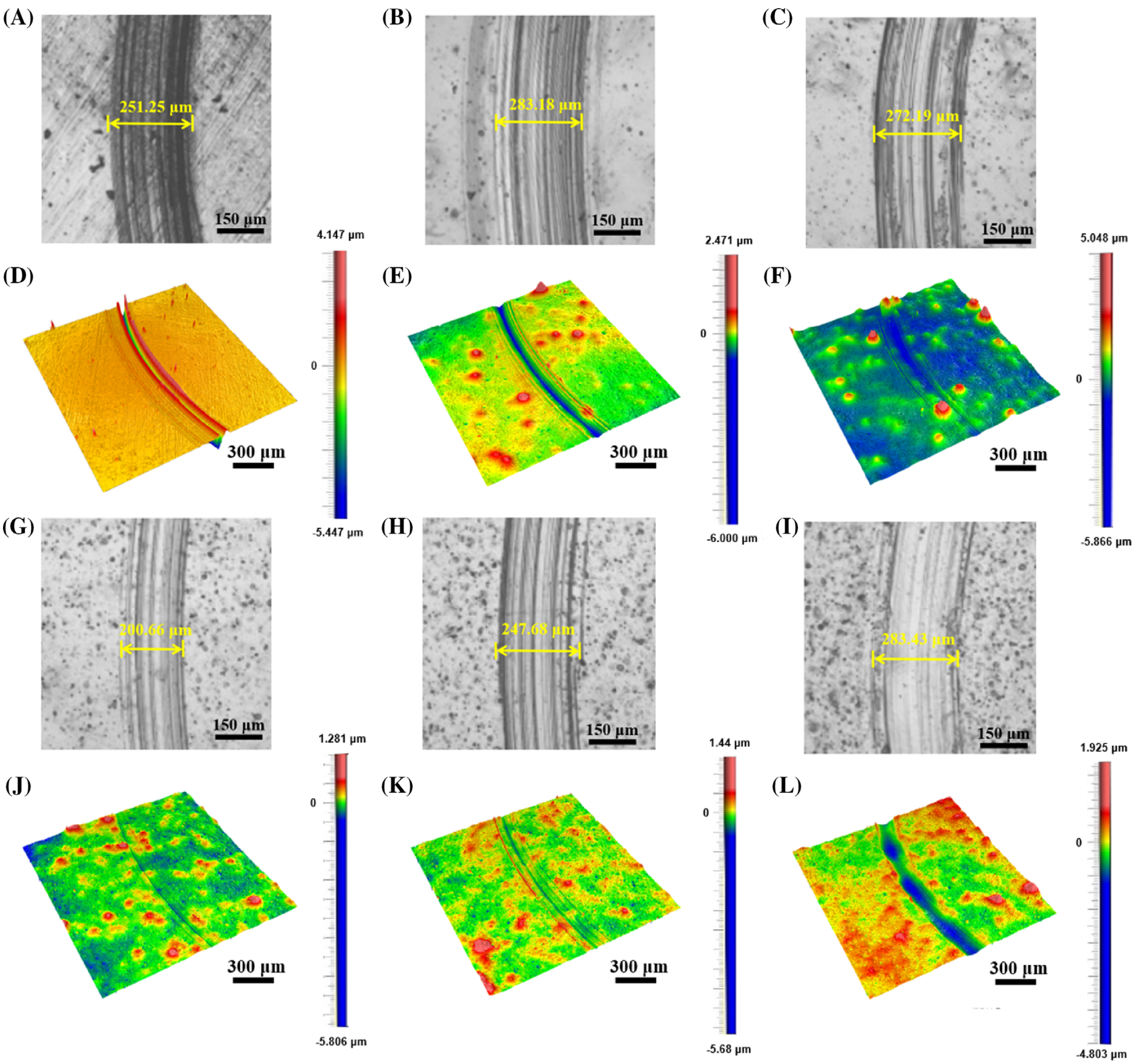

FIGURE 8 White light interferometric fringing intensity map (A–C), (G–I) and 3D morphology (D–F), (J–L) of the abrasion marks: (A, D) single PI; (B, E): MTPI-1; (C,F): MTPI-2; (G, J): MTPI-3; (H, K): MTPI-4; (I, L): MTPI-5.

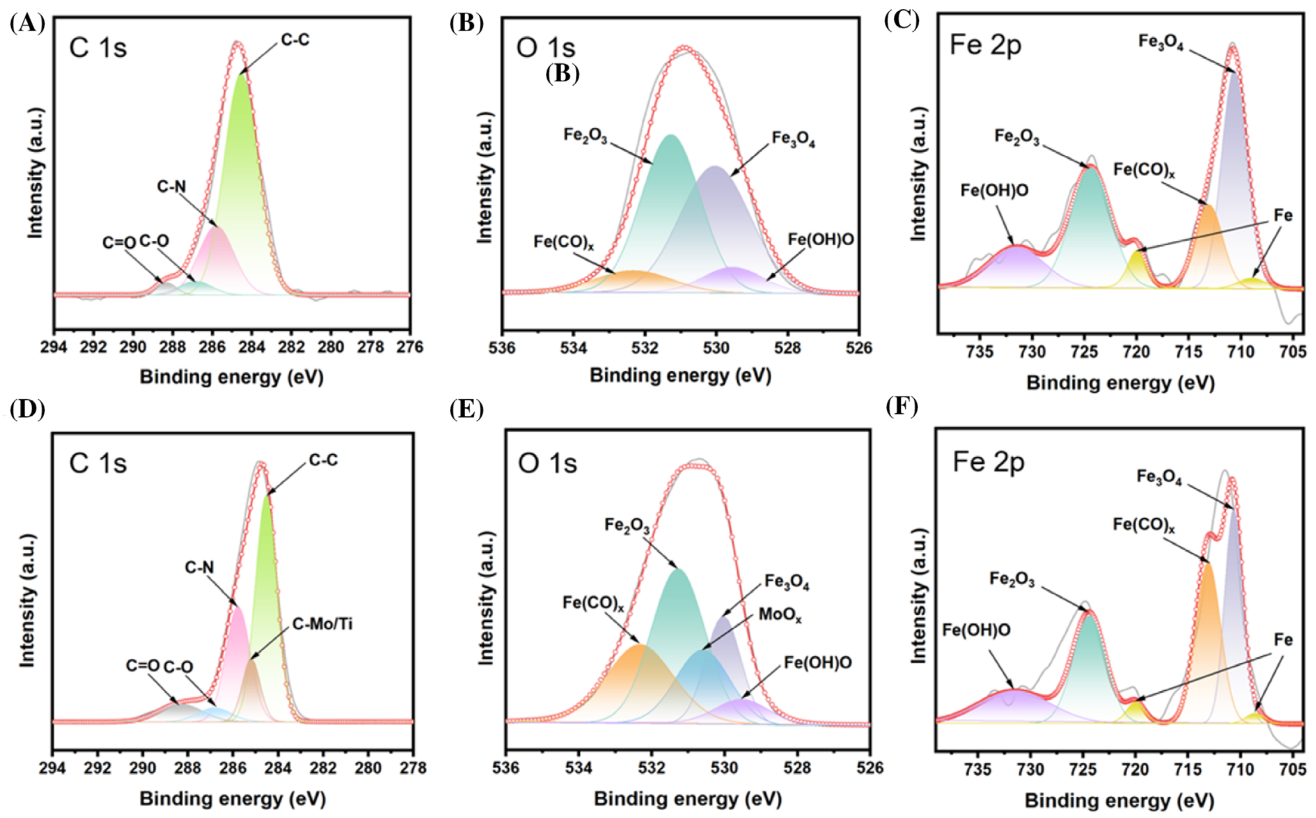

FIGURE 9 The x-ray photoelectron spectroscopy fine spectra of (A) C 1s (B) O 1s (C) Fe 2p of the transfer film formed by single PI and (D) C 1s (E) O 1s (F) Fe 2p of the transfer film formed by MTPI-3.

wear rate rises. When the content of $Mo_2Ti_2C_3$ reached 2.0 wt%, microcracks came into being on the surface of the abrasion marks (Figure S2f), illustrating that at this time the form of wear was dominated by abrasive grain wear and fatigue wear.

3.4 | Tribological mechanism analysis of $Mo_2Ti_2C_3$/PI composites

So as to better illustrate the wear mechanism, use XPS to characterize the transfer films formulated on the steel balls by single PI and MTPI-3 after friction wear experiments. The results are demonstrated in Figure 9. Figure 9A–C show the C, O, and Fe elemental fine spectra of the transfer film formed by single PI. In the C 1s fine spectrum, the peaks at 284.4, 285.8, 286.6, and 288.3 eV correspond to C—C, C—N, C—O, and C═O,[32] which proves that the PI was successfully passed on to the steel ball to generate a transfer film. In the O 1s fine spectrum peaks at 530.0 and 531.2 eV correspond to Fe_3O_4 and Fe_2O_3, respectively, which proves that an oxidation reaction occurred during the friction process, contributing to the generation of iron oxides on the steel balls, and the peaks at 724.3 and 710.6 eV in the Fe 2p fine spectrum further proves the generation of iron oxides.[33] The peaks at 532.3 eV in the fine spectrum of O1s and 713.2 eV in the Fe 2p fine spectrum, on the other hand, corresponded to the metal chelate $Fe(CO)_x$. The metal chelates have thermodynamic and thermal stabilizing properties, which can promote the stabilization of the transfer film and ameliorate the tribological properties.[34] In addition, peaks belonging to Fe(OH)O were also found.

Figure 9A,E–G show the XPS full spectrum and C, O, and Fe elemental fine spectra of the transfer film formed by MTPI-3. From the O 1s and Fe 2p fine spectra, we can find that the peak intensities belonging to Fe_2O_3 and Fe_3O_4 are lower after the addition of $Mo_2Ti_2C_3$, which proves that the addition of $Mo_2Ti_2C_3$ helps to reduce the oxidation of the friction surface. Meanwhile, the peak intensity of $Fe(CO)_x$ chelate is enhanced, which proves that the content of stable metal chelates in the transfer film is increased by the addition of $Mo_2Ti_2C_3$, which promotes the generation of continuous and stable transfer film. In addition, in the O 1s fine spectrum, the peak at 530.1 eV proves the generation of MoO_x, which has better self-lubricating ability, and its generation can better improve the tribological performances of the composites.

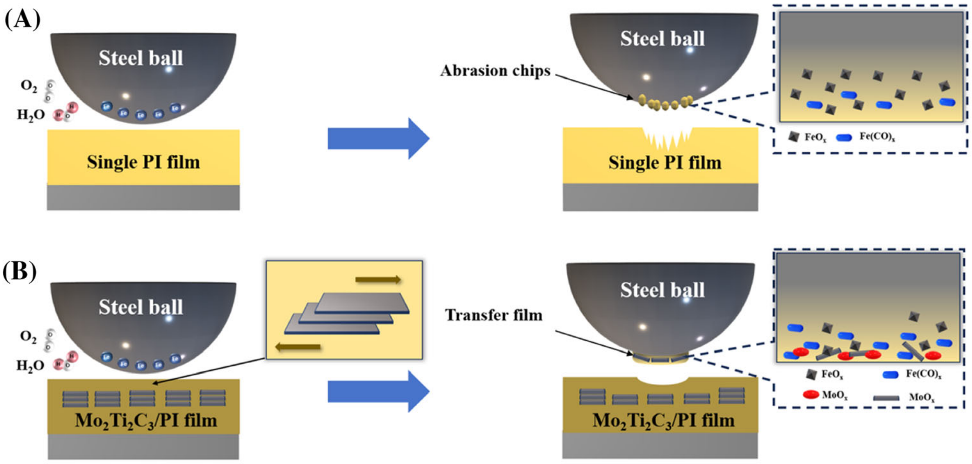

FIGURE 10 Diagrammatic sketch of the wear mechanism of (A) single PI and (B) $Mo_2Ti_2C_3$/PI composites.

On account of the above results and analysis, the reinforcement mechanism of $Mo_2Ti_2C_3$ on the tribological performances of is displayed schematically in Figure 10.

Figure 10A displays the wear mechanism of single PI. Single PI generates a large amount of abrasion chips when it receives shear stress and frictional heat. Then the abrasion chips transfer to the steel ball to produce a rough transfer film with many interruptions and gaps. After adding $Mo_2Ti_2C_3$, as shown in Figure 10B, the flake layer of $Mo_2Ti_2C_3$ is peeled off under the impact of shear stress and assists the PI matrix to generate a consecutive and glazed transfer film on the steel ball. This transfer film provides a smoother friction counterface, and the existence of MoO_x offers good self-lubricating properties. Therefore, the COF and the wear rate are reduced compared to single PI. In addition, under the influence of dry friction conditions, without the presence of a lubricating medium, the friction heat is difficult to dissipate. This makes the material more susceptible to heat and deterioration.[23] After the addition of $Mo_2Ti_2C_3$, the thermal stability number of PI is less affected by frictional heat during friction, which is aussichtsreich to the improvement of the tribological behaviors of the materials.

4 | CONCLUSION

In this work, single PI film was synthesized using ODA and BPDA, and a sequence of $Mo_2Ti_2C_3$/PI nanocomposite films were prepared by adjusting the additive amount of $Mo_2Ti_2C_3$ in the PI matrix. The tribological performances of single PI and $Mo_2Ti_2C_3$/PI composites were tested. The test results indicate that when the addition of $Mo_2Ti_2C_3$ was 1.2 wt%, the composites had the best tribological behaviors, and the COF and wear rate of the composites were cut down by 19.9% and 79.7% compared with single PI. This was due to the fact that the layered material $Mo_2Ti_2C_3$ MXene could assist the PI polymer to generate a smooth and consecutive transfer film on the steel ball. The transfer film has good self-lubricating properties, leading to preferable tribological behaviors of the material. This study demonstrates the excellent friction and wear resistance of $Mo_2Ti_2C_3$/PI nanocomposites, which broadens the adhibition field of PI composites and provides a reference for the application of two-dimensional layered material $Mo_2Ti_2C_3$ MXene as a solid lubricant.

AUTHOR CONTRIBUTIONS

Xinrui Wang: Writing–original draft, Conceptualization, Data curation, Investigation, Validation. **Guojing Chen:** Writing–revision draft, Conceptualization, Validation, Methodology. **Yufei Huang**, **Zhenqian Ma** and **Xuan Yin**: Investigation. **Chunpeng Chai**: Conceptualization, Funding acquisition, Investigation, Methodology, Project administration.

ACKNOWLEDGMENTS

In this work, some of the experiments were done at the Tsinghua University (Raman spectroscopic testing). The authors would like to thank Shiyanjia lab (www.shiyanjia.com) for the support of XRD and XPS tests.

CONFLICT OF INTEREST STATEMENT

The authors declare no conflicts of interest.

DATA AVAILABILITY STATEMENT

Data will be made available on request.

ORCID

Chunpeng Chai https://orcid.org/0000-0003-0334-9403

REFERENCES

1. Khosa MK, Jamal MA, Iqbal R, et al. Thermal stability and mechanical properties of organo-soluble and processable polyimides for high-temperature materials. *Polym-Plast Technol Eng*. 2017;56(1):22-28. doi:10.1080/03602559.2016.1185627
2. Zhang L-B, Wang J-Q, Wang H-G, et al. Preparation, mechanical and thermal properties of functionalized graphene/polyimide nanocomposites. *Compos Part A: Appl Sci Manuf*. 2012;43(9):1537-1545. doi:10.1016/j.compositesa.2012.03.026
3. Zhang D, Wang C, Qing T, Wang Q, Wang T. Research progress of porous polymer bearing retainer materials used in aerospace. *J Mech Eng*. 2018;54(9):17-26. doi:10.3901/JME.2018.09.017
4. Wang Y, Cai P, Wang T, Wang Q. Influence of graphite on tribological properties of hexagonal boron nitride hybrid/polyimide composites in wide temperature range. *J Tribol*. 2017;140(1):11605. doi:10.1115/1.4036935
5. Wan C, Zhan S, Jia D, et al. Tribological behavior of nanographite/polyimide composite under drying sliding condition. *Wear*. 2022;494–495:204271. doi:10.1016/j.wear.2022.204271
6. Yang M, Zhang C, Su G, Dong Y, Mekuria TD, Qingtao L. Preparation and wear resistance properties of thermosetting polyimide composites containing solid lubricant fillers. *Mater Chem Phys*. 2020;241:122034. doi:10.1016/j.matchemphys.2019.122034
7. Zhu L, You L, Shi Z, Song H, Li S. An investigation on the graphitic carbon nitride reinforced polyimide composite and evaluation of its tribological properties. *J Appl Polym Sci*. 2017;134(41):45403. doi:10.1002/app.45403
8. Min C, Liu D, Qian J, et al. High mechanical and tribological performance polyimide nanocomposites using amine-functionalized graphene nanosheets. *Tribol Int*. 2018;131:1-10. doi:10.1016/j.triboint.2018.10.013
9. Naguib M, Kurtoglu M, Presser V, et al. Two-dimensional nanocrystals produced by exfoliation of Ti_3AlC_2. *Adv Mater*. 2011;23(37):4248-4253. doi:10.1002/adma.201102306
10. Naguib M, Mochalin VN, Barsoum MW, Gogotsi Y. 25th anniversary article: MXenes: a new family of two-dimensional materials. *Adv Mater*. 2014;26(7):992-1005. doi:10.1002/adma.201304138
11. Meng F, Zhang Z, Gao P, et al. Excellent tribological properties of epoxy—Ti_3C_2 with three-dimensional nanosheets composites. *Friction*. 2021;9(4):734-746. doi:10.1007/s40544-020-0368-1
12. Bashandeh K, Amiri AS, Rafieerad A, et al. MXene-aromatic thermosetting copolyester nanocomposite as an extremely wear-resistant biocompatible implant material for osteoarthritis applications. *Appl Surf Sci*. 2022;600:154124. doi:10.1016/j.apsusc.2022.154124
13. Yin X, Pang H, Xu J, Liu D, Chai C, Zhang B. In situ-formed ultralow wear tribofilms induced by poly (acrylic acid)-co-MXene-modified polymer-like carbon films. *Adv Eng Mater*. 2022;24(7):2101661. doi:10.1002/adem.202101661
14. Gandla D, Zhang F, Tan DQ. Advantage of larger interlayer spacing of a $Mo_2Ti_2C_3$ MXene free-standing film electrode toward an excellent performance supercapacitor in a binary ionic liquid–organic electrolyte. *ACS Omega*. 2022;7(8):7190-7198. doi:10.1021/acsomega.1c06761
15. Fang Y, Feng Y, Liu X, Li C, Zhu J, Liu Y. Influence of Mo doping on the tribological behavior of Ti_3AlC_2 ceramic at different temperatures. *Ceram Int*. 2021;47(18):25520-25530. doi:10.1016/j.ceramint.2021.05.276
16. Saraf M, Chacon B, Ippolito S, et al. Enhancing charge storage of $Mo_2Ti_2C_3$ MXene by partial oxidation. *Adv Funct Mater*. 2023;34(1):2306815. doi:10.1002/adfm.202306815
17. Hua S, Huang B, Le Z, Huang Q. Mo-based $Mo_2Ti_2C_3$ MXene as photothermal nanoagents to eradicating methicillin-resistant Staphylococcus aureus with photothermal therapy. *Mater Des*. 2023;231:112033. doi:10.1016/j.matdes.2023.112033
18. Halim J, Cook KM, Naguib M, et al. X-ray photoelectron spectroscopy of select multi-layered transition metal carbides (MXenes). *Appl Surf Sci*. 2016;362:406-417. doi:10.1016/j.apsusc.2015.11.089
19. Tseng I-H, Chang J-C, Huang S-L, Tsai M-H. Enhanced thermal conductivity and dimensional stability of flexible polyimide nanocomposite film by addition of functionalized graphene oxide. *Polym Int*. 2013;62(5):827-835. doi:10.1002/pi.4375
20. Nie P, Min C, Song H-J, Chen X, Zhang Z, Zhao K. Preparation and tribological properties of polyimide/carboxyl-functionalized multi-walled carbon nanotube nanocomposite films under seawater lubrication. *Tribol Lett*. 2015;58(1):7. doi:10.1007/s11249-015-0476-7
21. Cao Z, Xie X, Chen X, et al. Wear- and high-temperature-resistant IGNs/ Fe_3O_4/PI composites for triboelectric nanogenerator. *J Electron Mater*. 2022;51(9):4986-4994. doi:10.1007/s11664-022-09752-y
22. Roy A, Mu L, Shi Y. Tribological properties of polyimide-graphene composite coatings at elevated temperatures. *Prog Org Coat*. 2020;142:105602. doi:10.1016/j.porgcoat.2020.105602
23. Chen B, Li X, Jia Y, et al. MoS_2 nanosheets-decorated carbon fiber hybrid for improving the friction and wear properties of polyimide composite. *Compos A: Appl Sci Manuf*. 2018;109:232-238. doi:10.1016/j.compositesa.2018.02.039
24. Vishal K, Rajkumar K, Sabarinathan P. Effect of recovered silicon filler inclusion on mechanical and tribological properties of polytetrafluoroethylene (PTFE) composite. *Silicon*. 2022;14:4601-4610. doi:10.1007/s12633-021-01250-w
25. Chen GJ, Ma ZQ, Jiang S, Wang XR, Huang YF, Chai CP. Highly lubricating and wear-resistant $Ti_3C_2Tx@SiO_2$/PI composites based on the action of transfer film at the friction surface. *Polym Compos*. 2024:1-12. doi:10.1002/pc.28200
26. Chai CP, Ma ZQ, Yin X, Pang HS. Self-lubricating and self-healing polyurethane nanocomposites based on aminated-Ti3C2Tx. *ACS Appl Polym Mater*. 2024;6:2513-2563. doi:10.1021/acsapm.3c02629
27. Zhao YL, Qi XW, Dong Y, et al. Mechanical, thermal and tribological properties of polyimide/nano-SiO_2 composites synthesized using an in-situ polymerization. *Tribol Int*. 2016;103:599-608. doi:10.1016/j.triboint.2016.08.018
28. Jin LY, Wang XR, Huang YF, et al. Chai lubrication mechanism of polyimide/V2CTx MXene composites based on surface chemistry. *Polym Compos*. 2023;44:8075-8084. doi:10.1002/pc.27689
29. Chen GJ, Jiang S, Huang YF, Pang HS, Yin X, Chai CP. Ultralow wear in multifunctional Ti3C2Tx/PI composite films induced by tribo-chemistry mechanism. *React Funct Polym*. 2023;193:105744. doi:10.1016/j.reactfunctpolym.2023.105744
30. Wan C, Yao C, Li J, et al. Friction and wear behavior of polyimide matrix composites filled with nanographite. *J Appl Polym Sci*. 2022;139(18):52058. doi:10.1002/app.52058
31. Qin S, Chen C, Cui M, Zhang A, Zhao H, Wang L. Facile preparation of polyimide/graphene nanocomposites via an in-situ

polymerization approach. *RSC Adv*. 2017;7(5):3003-3011. doi:10.1039/C6RA25168D

32. Hu C, Qi H, Yu J, Zhang G, Zhang Y, He H. Significant improvement on tribological performance of polyimide composites by tuning the tribofilm nanostructures. *J Mater Process Technol*. 2020;281:116602. doi:10.1016/j.jmatprotec.2020.116602
33. Huai Y, Plackowski C, Peng Y. The effect of gold coupling on the surface properties of pyrite in the presence of ferric ions. *Appl Surf Sci*. 2019;488:277-283. doi:10.1016/j.apsusc.2019.05.236
34. Pitenis AA, Harris KL, Junk CP, Blackman GS, Sawyer WG, Krick BA. Ultralow wear PTFE and alumina composites: it is all about tribochemistry. *Tribol Lett*. 2015;57(1):4. doi:10.1007/s11249-014-0445-6

SUPPORTING INFORMATION

Additional supporting information can be found online in the Supporting Information section at the end of this article.

How to cite this article: Wang X, Chen G, Huang Y, Ma Z, Yin X, Chai C. Tribological behavior and mechanism of $Mo_2Ti_2C_3$/polyimide composite films under dry friction condition. *Polym Compos*. 2024;1-12. doi:10.1002/pc.28317